*Journal of Applied Fluid Mechanics*, Vol. 9, No. 5, pp. 2475-2487, 2016.
Available online at www.jafmonline.net, ISSN 1735-3572, EISSN 1735-3645.
DOI: 10.18869/acadpub.jafm.68.236.25094

# Experimental and Numerical Investigation of Coating Effect on Pump Impeller and Volute

O. Kocaaslan[1], M. Ozgoren[2]†, M. H. Aksoy[2]and O. Babayigit[3]

[1]*Selcuk University, Huglu Vocational School, Huglu-Konya, Turkey*
[2]*SelcukUniversity, Engineering Faculty, Mechanical Engineering Department, Konya, Turkey*
[3]*Selcuk University Hadim Vocational School, Hadim-Konya, Turkey*

†*Corresponding Author Email:mozgoren@selcuk.edu.tr*

(Received May 20, 2015; accepted December 2, 2015)

## ABSTRACT

In this study, an impeller and volute of a centrifugal pump were designed and numerically analyzed in order to improve the pump efficiency. Before design, experimental and theoretical studies were performed on a centrifugal water pump taken as Model Pump (MP). Design parameters were taken as 100 $m^3/h$ for volume flow rate, 18m for head and 1480 rpm for rotating speed. After the inspection of the flow field in the MP, some geometrical modifications such as impeller inlet and outlet diameters, blade inlet and exit angles, blade wrap angle, blade thickness, blade inletand exit widthswere realized to design a new pump. Numerical analyses were performed for 8 different volume flow rates overlapping with experimental operation points by Ansys-Fluent Software. In numerical studies, k-ε turbulence model and standard wall function were utilized. The experimental and computational results were compared with the model pump. According to the analysis results at design flow rate, hydraulic torque value is decreased from 56.62 Nm to 51.05 Nm, while hydraulic efficiency is increased from 55.98% to 63.09%. In addition, in order to see the roughness effect and increase the pump efficiency, the wetted surfaces of the impeller and volute were coated with a polyurethane dye material. Later, performance curves of the coated and uncoated pumps were experimentally obtained which showed that the shaft power of the pump for the coated case was decreased around 10% and the hydraulic efficiency of the pump was increased approximately 18%. According to the economic analysis by basic payback period of the polyurethane coating is less than one year and the internal income ratio for ten-year life-cycle period is around %114.

**Keywords**: Centrifugal pump; CFD; Coating; Hydraulic efficiency;k-ε turbulence model;Polyurethane coating;Turbulence kinetic energy.

## NOMENCLATURE

| | | | |
|---|---|---|---|
| $A$ | cross-section area | $P_s$ | shaft power |
| $C$ | investment cost | $\dot{Q}$ | flow rate |
| $C_{1\varepsilon}$, $C_{2\varepsilon}$ , $C_\mu$ | constants in the turbulence equations | $r$ | internal income ratio |
| | | $S$ | yearly total saving |
| $g$ | gravitational acceleration | $S_{ij}$ | strain rate tensor |
| $G_k$ | generation of turbulence kinetic energy (due to mean velocity) | $S_k$, $S_\varepsilon$ | user-defined source terms |
| | | $T_h$ | torque |
| $G_b$ | generation of turbulence kinetic energy (due to buoyancy) | $V$ | voltage |
| | | $w$ | angular velocity |
| $H_m$ | head | $w_{\eta h}$ | uncertainty of hydraulic efficiency |
| $I$ | electric current | | |
| $i$ | interest ratio | | |
| $k$ | turbulent kinetic energy | $\eta_{em}$ | electrical motor efficiency |
| $K$ | constant of flow velocity | $\eta_h$ | hydraulic efficiency |
| $\dot{n}$ | rotating speed | $\mu_t$ | dynamic eddy viscosity |
| $N_s$ | specific speed | $\sigma_k$, $\sigma_\varepsilon$ | turbulent Prandtl number for k and ε |
| $P$ | present value | | |
| $cos\varphi$ | power factor | $DP$ | designed pump |
| $\rho$ | density | $IRR$ | internal rate of return |
| $CFD$ | computational fluid dynamics | $PBP$ | basic payback period |

| | | | |
|---|---|---|---|
| *CMP* | coated model pump | *MP* | model pump |
| $P_e$ | electrical power | *NPV* | net present value |
| $P_h$ | hydraulic power | | |

## 1. INTRODUCTION

Centrifugal pumps are widely used for the purpose of water supply, hydrofor pump systems, industrial machines, waste pump, mud and irrigation systems, water treatment, HVAC applications and many more in daily life. Approximately 20% of the electricity consumed in the world has been used in the pump energy supply while around 10% of Turkey's electricity consumption is used by pumps and other turbo machineries (Perez *et al.* 2010;Golcu*et al.* 2006). In order to decrease this consumption ratio, even a very small percentage of efficiency improvement for pumps can provide significant amount of energy savings.

In recent years, it has gained great importance in improving efficiency of pumps with developing computer technology such as examination of the flow with numerical techniques. Time, material and labor losses of manufacturing realized with traditional methods are reduced with Computational Fluid Dynamics (CFD) on pump design studies (Dai *et al.* 1997). There are some studies about CFD application in pumps as follows.

Kaya and Aydın (2009) performed a 3-D CFD study on horizontal shaft, single-stage end-suction centrifugal pump in order to determine the characteristics for different flow rates. Different turbulence models and different working fluids were also examined. Babayigit *et al.* (2015) investigated the effect of the blade inlet angle variation on hydraulic efficiency of the centrifugal pump impeller when the impeller inlet and outlet widths, blade number and blade thicknesses were kept constant. According to the CFD analysis, the impeller blade inlet angles on hub were changed from 17° to 30°. For the best efficiency point, impeller blade inlet angle was found to be 27°. Jafarzadeh *et al.* (2010) presented a three-dimensional simulation of turbulent fluid flow to predict velocity and pressure fields for a centrifugal pump. They used a commercial CFD code to solve the governing equations of the flow field. They applied three turbulence models which were standard k–ε, RNG and RSM. They compared their simulation results of the pump characteristics curves and experimental data. Li (2011a) performed a study on the effects of the blade discharge angle on the performance of an industrial centrifugal oil pump. The results showed that the blade discharge angle has a great influence on the head, shaft power and efficiency of the centrifugal pump.

In applications, there can be a decrease in efficiency due to erosion, corrosion, cavitation, and deposits that increase friction on the internal surfaces of the pump. The increased resistance to flow decreases the pump efficiency. This expected degradation of the pump performance can be halted with the use of coating on pump surfaces (Maillard 2008; Xia 2002).There are also some studies on roughness effect on the pump surfaces and coating effect on the pump performance. Bellary and Samad (2013) investigated the exit blade angle and impeller surface roughness on the performance of a centrifugal pump impeller. Standard k-ε with two equation models was used for the turbulent closure of steady incompressible flow. The investigation pointed out that the blade exit angle had an influence on the head, shaft power and efficiency of the impeller for different liquids. Rise in head, increase in shaft power and decrease in hydraulic efficiency were observed with increasing roughness. Li(2011b) examined the effect of blade exit angle and viscosity as well as the roughness on the performance of the centrifugal pump with a developed CFD code.

The aim of this study is to design numerically and validate experimentally an impeller and volute of a model centrifugal pump in order to improve the pump efficiency. A polyurethane coating was also applied on the wetted surface of the pump to see the effect of roughness and coating on the hydraulic efficiency and performance curves, which were not encountered on a impeller-volute interaction of the centrifugal pump in the literature.

## 2. MATERIALS AND METHOD

The MP called as TKF 80-250 was examined in this study which is currently manufactured by Sempa Pump Co. in a mass production line. Firstly, performance curves of the MP were performed in a pump test rig without any modification on the pump impeller and volute with original shape. In order to polish the wetted surfaces and decrease the roughness effect, a polyurethane coating process was applied to the model pump and then the polyurethane Coated Model Pump (CMP) was generated and tested. In addition, the MP was also analyzed by CFD to compare the results with experimental data. In the generation of the pump model, in order to simulate the real working conditions, balance holes and leakage losses of the MP were also included as shown in Figs. 1 and 2, which was a distinguished part of this study from the literature. After the CFD analysis of the MP, flow characteristics in the flow field were sensitively investigated and compared with the experimental data. Flow separation, intensive turbulent kinetic energy, low pressure regions and flow structures were determined to modify the geometry of the impeller and volute of the MP. Furthermore, some geometrical modifications such as impeller inlet and outlet diameters, blade inlet and exit angles, blade wrap angle, blade inlet and exit widths, blade thickness were realized to design a new pump. This new Designed Pump is presented as designed pump (DP) in the text and numerical results of the DP were also investigated in this study.

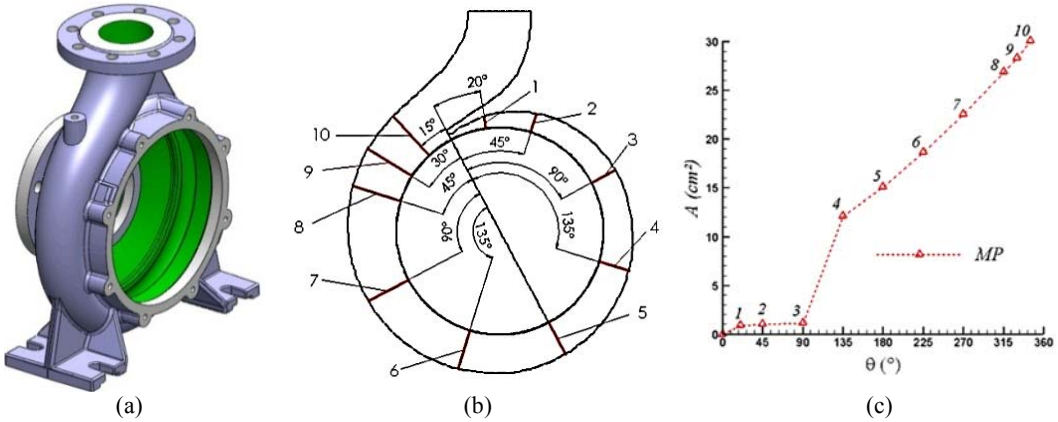


(a) (b) (c)

**Fig. 1. (a) MP's solid model, (b) cross-section area variations and (c) their magnitudes area in cm$^2$ versus angles around the volute.**

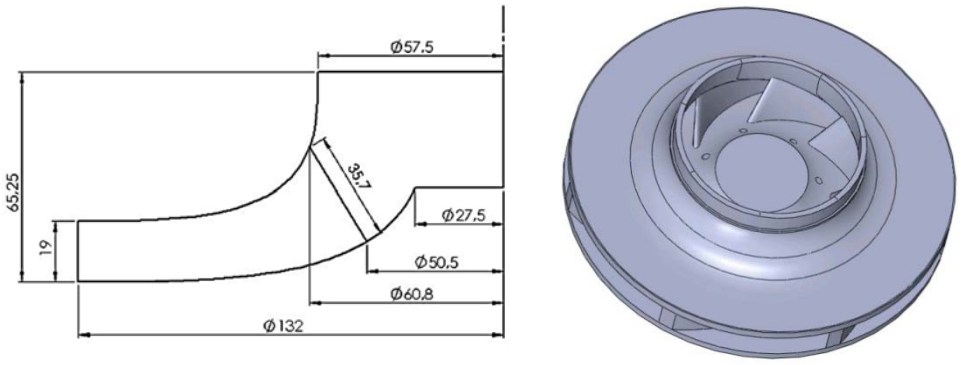


**Fig. 2. Meridional profile and solid model of the MP's impeller.**

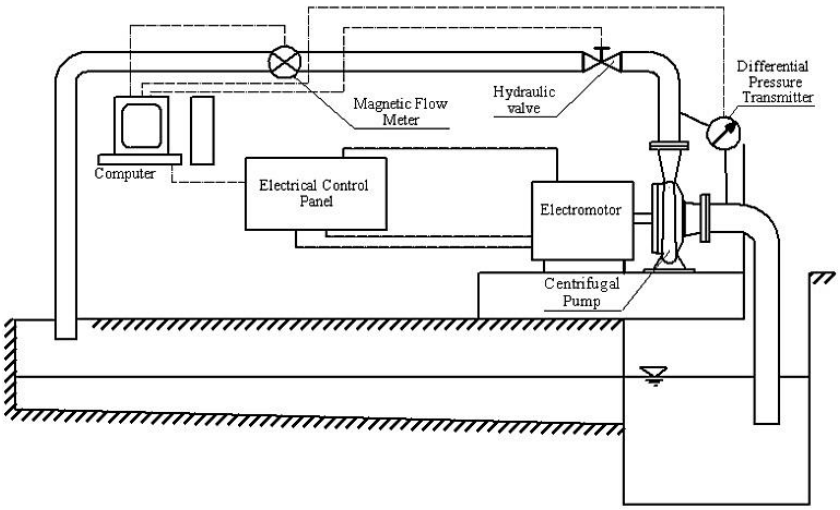


**Fig. 3. Experimental setup for the pump.**

## 2.1 Experimental Study

The MP and CMP were tested by a centrifugal pump performance test rig that was established according to the standard TS EN ISO 9906 is schematically shown in Fig. 3. In the test rig, the pressure was measured by a differential transmitter at the suction and discharge of the tested pump A calibrated magnetic flow meter was used to measure the flow rate and an electricity control panel was used to determine the electric consumption amount of the pump in different flow rates and shaft rotation speeds. Accuracy values of the measurement devices are given in Table 1.

Experiments were separately repeated for the different flow rates by adjusting the throttle valve. The values read from the volume flow meter,

differential pressure transmitter and electrical control panel were recorded and processed. After experimental studies were performed, the hydraulic power ($P_h$) and the hydraulic efficiency ($\eta_h$) of the pumps were calculated using manometric pressure height ($H_m$) in m unit, volume flow rate ($\dot{Q}$) in $m^3/s$. The equations used for the calculations were as follows (Kocaaslan 2015):

$$P_h = \frac{\rho g \dot{Q} H_m}{1000} \quad (1)$$

$$P_e = \frac{\sqrt{3}\, VI\, cos\varphi}{1000} \quad (2)$$

$$P_s = \eta_{e.m}\eta_m P_e \quad (3)$$

$$\eta_h = \frac{P_h}{P_s} \quad (4)$$

The efficiency of the electric motor and all mechanic loses were taken from the manufacturer of the motor according to loading percentage and also taken into account in experiments.

**Table 1 Measurement parameters and their accuracy values**

| Measurement parameters | Accuracy (%) |
|---|---|
| Pressure transmitter (Pa) | ±0.05 |
| Flow rate ($m^3/h$) | ±0.04 |
| Electric Current (A) | ±0.1 |
| Voltage (V) | ±0.1 |
| Cosφ | ±0.1 |
| Revolution of the pump (rpm) | ±0.1 |

In the experimental studies, uncertainties occur because of the fact that various errors exist from measuring equipment, the surrounding environment and human errors from the person doing the experiments. In every experiment, the hydraulic efficiency uncertainty, $\omega_\eta$, caused by different independent variables can be expressed as in Eq.(5) (Holman 2001). The uncertainty values reflect the specifying effects of total errors for the measured quantities, achieving more accurate measurements and assisting in reducing the uncertainties.

$$w_{\eta_h} = \pm\left[\left(\frac{\partial \eta_h}{\partial P}\omega_P\right)^2 + \left(\frac{\partial \eta_h}{\partial \dot{Q}}\omega_{\dot{Q}}\right)^2 + \left(\frac{\partial \eta_h}{\partial I}\omega_I\right)^2 + \left(\frac{\partial \eta_h}{\partial V}\omega_V\right)^2 + \left(\frac{\partial \eta_h}{\partial \phi}\omega_\varphi\right)^2\right]^{\frac{1}{2}} \quad (5)$$

Here, $\eta_h$ presents the calculated hydraulic efficiency amount using Eqs. 1 and 4. Variables $\omega_Q$, $\omega_P$, $\omega_I$ and $\omega_V$ show, respectively, accuracy values of the measurement devices for volume flow rate, manometers, ampere meter and voltmeter while $\omega_\eta$ is total uncertainty amount (±%) of dependent variable of hydraulic efficiency for the calculation derived from the measured values. Other parameters in Eqs. 1 and 4 were assumed to be constant. Variation of relative uncertainty against volume flow rate is given in Fig. 4. Uncertainty values of hydraulic efficiency in Eq. (5) depending on the measurement devices and parameters such as pump inlet and outlet pressures, volume flow rate, water density, electric current, voltage and electric motor efficiency were found to be less than ±1%. Continuing decreasing of the uncertainty values occurs due to the fact that volume flow rate increment is more dominant on the calculation of the hydraulic efficiency than the other measurement parameters including even high magnitudes of outlet pressure.

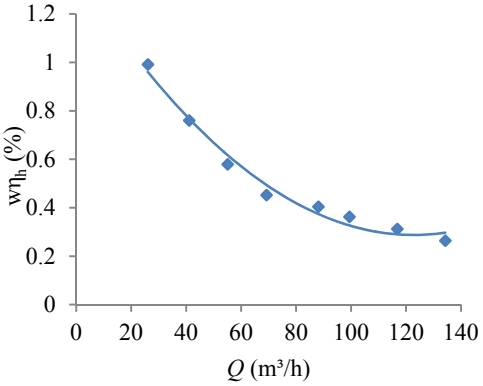


**Fig. 4. Variation of uncertainty against volume flow rate.**

## 2.2 Polyurethane Coating

One of performance effecting parameters on the pump efficiency is surface roughness. In order to decrease the roughness effect, manufacturing process to generate more refined wetted surfaces can improve the efficiency but it is still not easy due to the complex flow passage of the centrifugal pump components. In this study, surface roughness effect on the hydraulic efficiency is investigated for the MP. In order to provide easier roughness decrement method in this study, an industrial application with a polyurethane coating was applied for all wetted surfaces of the impeller and volute of the MP. Thickness of the polyurethane coating is around 0.75mm and material properties are given in Table 2. The balance holes on the impeller were drilled after the coating process. The coated pump (CMP) was tested to compare the performance curves with uncoated one (MP). In addition, coating provides cavitation resistant by a lower cost, better option than changing to a cavitation resistant material, such as stainless steel (Budris 2012). Some photographs during polyurethane coating process are presented in Fig. 5.

**Table 2 Technical properties of Polyurethane coating material (Anonymous,2014)**

| | |
|---|---|
| Density ($g/cm^3$) | 1.05 |
| Tensile strength ($N/mm^2$) | 24 |
| Tensile modulus (at 100% elongation) | 13 |
| Tear strength (N/mm) | 68 |
| Thermal conductivity (W/K.m) | 0.2 |
| Processing temperature (°C) | +120 |

## 2.3 Economic Analysis

Economic analyses were performed for the coating application of the CMP. Basic Payback Period (PBP), Net Present Value (NPV) and Internal Rate of Return (IRR) methods were applied for economic

evaluation.

**Fig. 5. Photographs of polyurethane coating process.**

A common and simple way to evaluate the economic merit of an application is to calculate its PBP. The unit of this value is in years and shows amount of the minimum time to recover the total investment as seen in Eq. (5) (Kose *et. al* 2014).

The NPV is a method that takesinto account the time value of money to assess long-term applications. All future income, saving and expenditure flows are discounted to the present (Ozerdem *et al.* 2006). The NPV is calculated as Eq. (6):

The IRR is a widely used method for the preliminary evaluation of projects and applications. The IRR method requires discount rate value r, which makes equal the NPV and the value of the cost and benefit (Ozerdem *et al.* 2006). In other words, it is the rate, which makes NPV equal to zero.

In the calculation, electric energy price for agricultural irrigation purpose which was cheaper than industrial one and in home usage was taken as 0.0783 USD/kWh in Turkey. Investment cost of the polyurethane coating was approximately 200 USD for the wetted surface of the impeller and volute including material and labor cost. Operating time of the centrifugal pump was assumed to be 8 hours per day for the calculation of energy consumption and saving.

$$PBP=C/AS \tag{5}$$

$$P = S\frac{(1+i)^n-1}{(1+i)^n\, i} \tag{6}$$

$$P = S\frac{(1+r)^n-1}{(1+r)^n\, r} \tag{7}$$

In the above equations, C is the investment cost of the polyurethane coating, S is yearly total saving, P is present value, i is the interest ratio and r is the internal income ratio.

## 2.4 Numerical Analysis

The CFD analysis was done after the MP was experimentally tested. The fluid domains of the centrifugal pump were generated including balance holes to take into consideration the leakage losses. Solid models of the MP and the fluid domains consisting of volute, inlet, outlet and impeller regions are shown in Fig. 6 and Fig. 7, respectively. Flow volume domains were meshed with tetrahedral cells. Calculation time of numerical analysis for complex geometry can be decreased with a suitable grid generation. Improvements in the solution grid or chosen small cells can provide closer numerical results to the experimental ones but they require larger storage place and time for the numerical solution. In this study, four different solution grids were formed and the most suitable grid structure was obtained. Cell numbers and numerical analyses results are given in Table 3. Results of the fluid domain with Meshes III and IV were very close to each other and also with experimental results in head and hydraulic efficiency. Due to the lower mesh number, the Mesh III structure was selected to carry out the numerical simulation in the flow volume as seen in Table 3.

**Table 3 Mesh Size Information**

| Computational Domain | Grid Number | $H_m$ (m) | $\eta_h$ (%) |
|---|---|---|---|
| Mesh I | $9.8 \times 10^6$ | 19.21 | 59.17 |
| Mesh II | $16.2 \times 10^6$ | 19.01 | 58.80 |
| Mesh III | $24.8 \times 10^6$ | 18.03 | 55.98 |
| Mesh IV | $31.8 \times 10^6$ | 18.01 | 55.62 |
| Experimental Results | - | 17.54 | 54.44 |

The boundary conditions are considered with the real operation conditions, as summarized in Table 4 and the boundaries on the model are shown in Fig. 9. Mass flow rate is specified in the pump inlet and pressure outlet boundary is used at the impeller outlet. Average surface roughness of the wetted surfaces was defined as 0.3 mm on hub, shroud, impeller surfaces and volute walls (i.e. wetted surfaces of the pump) which were taken from measurements of the manufactured impellers by sand casting method. Non-slip wall conditions were imposed overall the physical surfaces, except the interfaces between different parts. Maximum residuals are set to $10^{-5}$ and the mass flow rate value and static pressure value at the pump inlet and outlet are also monitored. When the overall imbalance of the four monitors was less than 0.1% or the maximum residuals were reached, the simulation was considered to be converged.

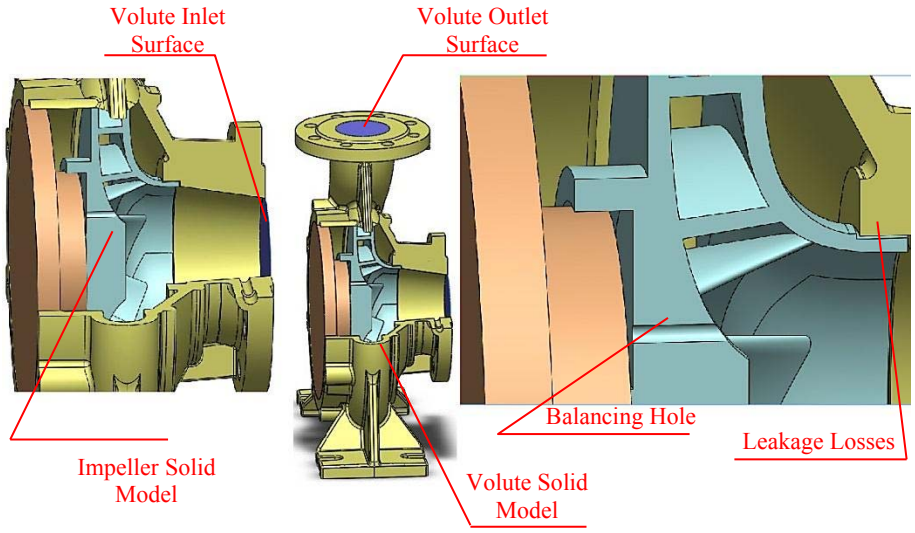


**Fig. 6. Solid models of the MP.**

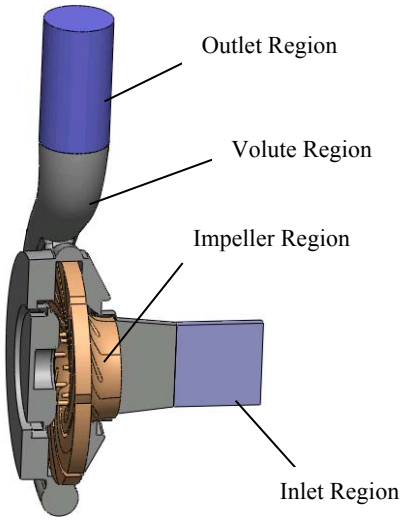


**Fig. 7. Flow volume of the model pump.**

**Table 4 Boundary conditions**

| Surface/Volume | Boundary conditions |
|---|---|
| Inlet | Mass flow rate |
| Hub, shroud, blades, walls of impeller region and wall volute | Non-slip condition |
| Impeller | Rotating reference frame |
| Outlet | Head |
| Wall function | Standard wall function |

The CFD code was solved for fully 3-D incompressible Navier-Stokes equations, including the centrifugal force effects in the impeller and the steady terms. Turbulence was simulated with the realizable k-ε model. For three-dimensional incompressible, steady flow, the continuity and momentum equations are written as follows (Anonymous 2015):

$$\nabla \vec{V} = 0 \tag{8}$$

$$\rho\nabla(\vec{v}\vec{v}) = -\nabla P + \mu\nabla^2\vec{V} + \rho\vec{g} + \vec{F} \tag{9}$$

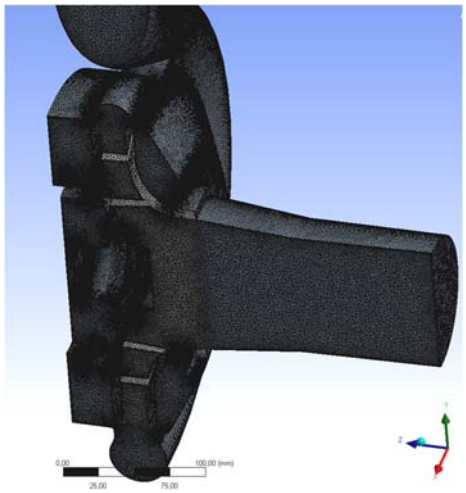

**a) General appearance of the grid structure**

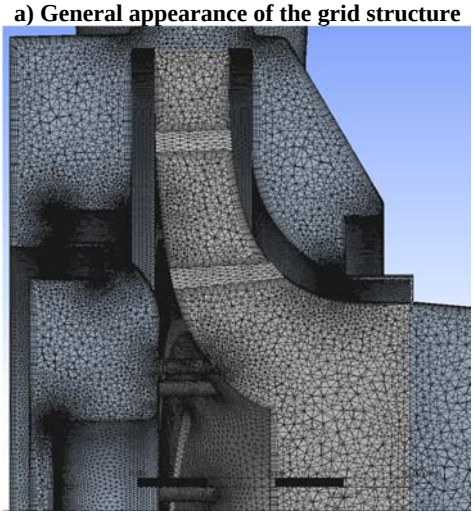

**b)Detailed view**

**Fig. 8. Grid structure for numerical simulations of the model pump.**

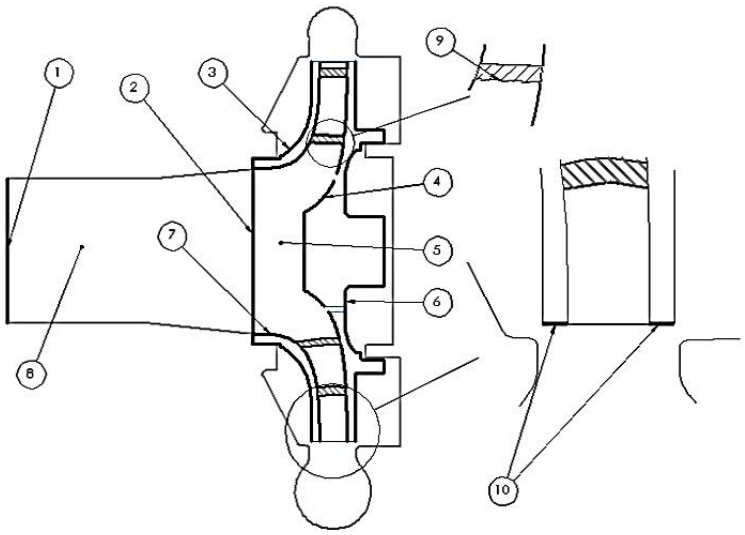


| | | | | | |
|---|---|---|---|---|---|
| **1** | Inlet | **5** | Impeller volume | **9** | Blade |
| **2** | Impeller Inlet | **6** | Hub surface of impeller solid model | **10** | Blade surface of impeller solid model |
| **3** | Shroud surface of impeller solid model | **7** | Shroud | | |
| **4** | Hub | **8** | Volute volume | | |

**Fig. 9. Surfaces and flow volumes of the pump.**

Transport equations for the realizable k - ε model (Anonymous 2015):

$$\frac{\partial}{\partial x_i}(\rho k u_j) = \frac{\partial}{\partial x_i}\left[\left(\mu + \frac{\mu_t}{\sigma_k}\right)\frac{\partial k}{\partial x_j}\right] + G_k + G_b - \rho\varepsilon - Y_M + S_k \quad (10)$$

$$\frac{\partial}{\partial x_i}(\rho \varepsilon u_j) = \frac{\partial}{\partial x_i}\left[\left(\mu + \frac{\mu_t}{\sigma_\varepsilon}\right)\frac{\partial \varepsilon}{\partial x_j}\right] + \rho C_1 S\varepsilon - \rho C_2 \frac{\varepsilon^2}{k+\sqrt{v\varepsilon}} + C_{1\varepsilon}\frac{\varepsilon}{k}C_3 G_b + S_\varepsilon \quad (11)$$

where

$$C_1 = max\left[0.43\frac{\eta}{\eta+5}\right] \quad (12)$$

$$\eta = S\frac{k}{\varepsilon} \quad (13)$$

$$S = \sqrt{2S_{ij}S_{ij}} \quad (14)$$

Here, $G_k$ represents the generation of turbulence kinetic energy due to the mean velocity gradients, $G_b$ is the generation of turbulence kinetic energy due to buoyancy, $Y_M$ represents the contribution of the fluctuating dilatation of incompressible turbulence to the overall dissipation rate, $C_2$ and $C_{1\varepsilon}$ are constants, $\sigma_k$ and $\sigma_\varepsilon$ are the turbulent Prandtl numbers for k and ε, respectively. $S_k$ and $S_\varepsilon$ are user-defined source terms. The standard values of different constants appearing in equations $C_{1\varepsilon}$=1.44, $C_2$=1.9, $\sigma_k$=1.0, $\sigma_\varepsilon$=1.2. Solution of Eqs. (10)and(11) give spatial variations of k and ε which, in turn, can be used to find out variation of turbulent viscosity or eddy viscosity $\mu_t$ using the Prandtl–Kolmogorov relation (Anonymous 2015):

$$\mu_t = \rho c_\mu \frac{k^2}{\varepsilon} \quad (15)$$

Hydraulic power and hydraulic efficiency were calculated using the numerical data from the Eqs.1 and 4 while Eqs. 16 and 17 were used to calculate shaft power and angular velocity, respectively (Cengel and Cimbala 2006).

$$P_s = \frac{T_h\,\omega}{1000} \quad (16)$$

$$\omega = \frac{\dot{n}\,\pi}{30} \quad (17)$$

where$\omega$ is the angular velocity in rad/s, $\dot{n}$ is revolution in rpm and $T_h$ is torque value in Nm (Baysal 1979).

## 2.5 Impeller and Volute Design

The volume flow rate of Q=100 $m^3$/h, 18m head height and 1480 rpm were taken as design parameters for the DP. Empirical formulas were used to determine the dimensions of the DP taken from Gulich (2014). Reynolds number at design volume flow rate at the inlet and outlet pipes were respectively calculated as Re=ρVD/μ=440155 and Re=352124. Here water density ρ=1000 kg/m3, V is mean velocity at the inlet or outlet, D is the pipe diameter at the inlet (0.08 m) or outlet (0.1m) and μ is dynamic viscosity μ=0.001 kg/ms. The volume flow rate were changed from 26 m3/h to 134, 28 m3/h for the analysis and the corresponding Reynolds numbers are in the range of Re=114616-591040 at the inlet and Re=91693-472832 at the outlet. .Blade inlet and outlet angles were found from well known velocity triangle rules. The geometry of the blade was generated by BladeGen software. For designing of the volute, Stepanoff theory was used (Stepanoff 1957). Reference point for the volute design was taken as zero degree at the volute tongue region, cross-section area of the gap

between volute and impeller was calculated by using the following Eqs. (18) and (20). Cross-section of the flowing area for the volute design from the volute tongue is taken as it increases linearly. In this manner, the average flow velocity between the outlet side of the impeller and the volute inner surfaces were kept constant while changing the cross-section area of the volute, and thus probability of the flow separation occurrence was considerably decreased (Stepanoff 1957).

$$K = \frac{2.18}{N_S^{0.32}} \tag{18}$$

$$V = K\sqrt{2gH_m} \tag{19}$$

$$A(\theta) = \frac{\dot{Q}}{V}\frac{\theta}{360} \tag{20}$$

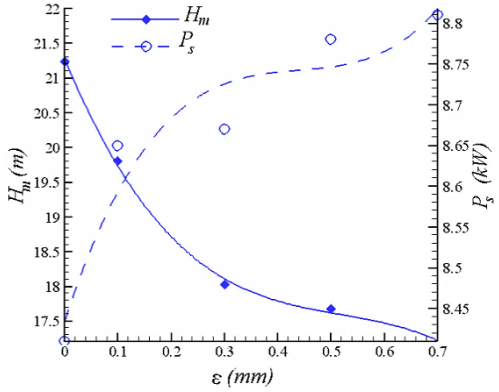


**Fig. 10. Variation of head and the shaft power at different roughness heights for the MP by CFD.**

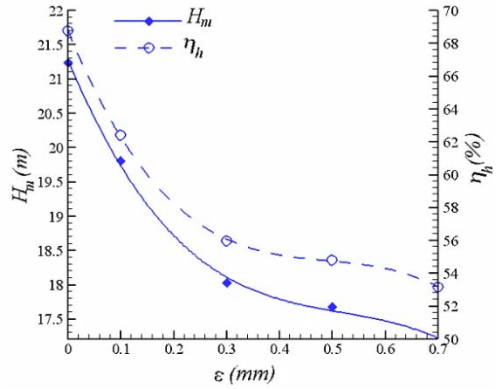


**Fig. 11. Variation of head and hydraulic efficiency at different roughness heights for the MP by CFD.**

## 3. RESULTS AND DISCUSSION

### 3.1 Experimental and CFD Results for MP and CMP

Roughness effect on the performance of the MP for the roughness values of 0, 0.1, 0.3, 0.5 and 0.7 mm on the wetted surfaces was analyzed by CFD using ANSYS-FLUENT for the design flow rate $100 m^3/h$ as seen in Fig. 10. As seen shaft power increases while head of the pump decreases by increasing roughness heights. It was also found that the hydraulic efficiency was decreased from 68% to 53% as the roughness value increased from 0 to 0.7 mm as shown in Fig.11.

Performance characteristics of the CMP and MP were determined by experimental studies and presented in Figs. 12 and 13.

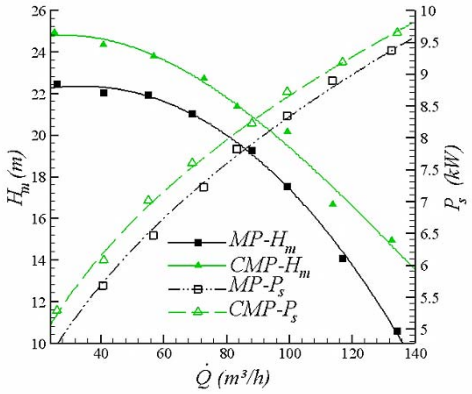


**Fig. 12. Comparison of the head and the shaft power for the CMP and MP by experimental data.**

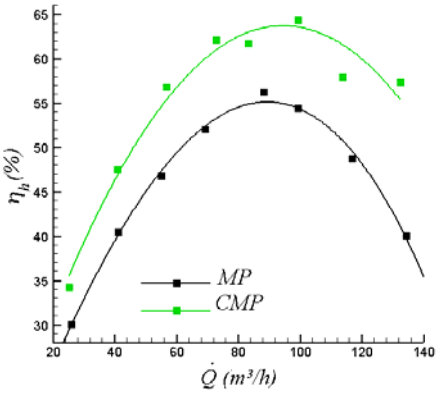


**Fig. 13. Comparison of the hydraulic efficiencies of the CMP and MP experimental resultsby experimental data.**

It was demonstrated that head and corresponding hydraulic efficiency of the CMP were considerably increased comparing with the MP. For example, the heads and corresponding hydraulic efficiencies for the CMP/MP at $100 m^3/h$ were obtained as 20.2 m / 17.6 m and 64.3% / 54.4%, respectively. The reason of this efficiency improvement is that the decrement of the surface roughness although coating application decreases the flow passage in the impeller. At design flow rate, electric consumption of the MP and CMP were found to be 9.67 kWh and 9.26 kWh, respectively. According to these results from Eq. (5), yearly energy saving amount was found to be 174 US dollars and the PBP was calculated as 0.87 years. NPV for interest ratio of 0.1 and 10 years life-cycle period of the polyurethane coating from Eq.(6)yields 1404.83 USD that is tremendously larger than the investment cost value of 200 USD. Similarly, the

IRR ratio calculated by Eq. 6) was found to be %114 so that coating can be applied feasibly.

### 3.2 Comparison of the CFD and Experimental Results

Head and hydraulic efficiency variations obtained by CFD and pump test rig of the MP are presented in Fig. 14. The head was calculated by the total pressure difference at the outlet and inlet surfaces of the pump. Hydraulic torque was computed through the rotational flow volume of the pump along the curved surfaces and then hydraulic efficiency was calculated. Performance characteristics are similar for the CFD and experimental results in Fig. 14. The hydraulic efficiency increased with the volume flow rate until the design flow rate, and then it tended to decrease. At this flow rate, the head values were found to be 18.0 m and 17.6 m for CFD and experimental results, respectively. These values were in a close agreement. Relative difference between the CFD and experimental results were respectively found to be 2.79% and 2.82% for the head and hydraulic efficiency on design flow rate which was acceptable value when compared to the literature (Yang *et al.* 2012; Zhou *et al.* 2012). It is proven that the CFD yield trustable results and thus a new pump model can be studied only numerically without experimental tests. In order to improve the efficiency of the MP some geometric changes are applied and a new pump is generated.

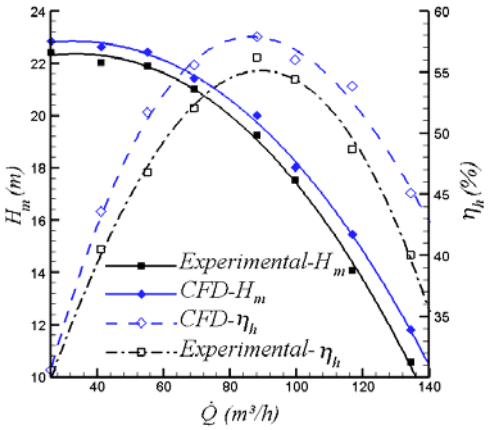


**Fig. 14. Comparison of the experimental and CFD resultsfor the MP.**

### 3.3 Comparison of the Designed Impeller and Volute

After the inspection of the flow field in the MP, some geometrical modifications were made to design the DP. After many trials and analyses, impeller exit diameter, impeller entrance diameter, blade entrance and exit angles, blade wrap angle, blade entrance and exit widths, blade thickness of the MP were changed as seen in Table 6. The cross-section area variations of the MP and DP between the outlet of the impeller and the volute inner surfaces through the centrifugal pump are shown in Fig. 15. The DP has more linear cross-sectional are a distribution than the MP. Meridional sections of the impeller and volute profiles for the MP and DP are shown in Fig. 16. It is seen that meridional section of the DP has narrower flow stream way than that of the MP.

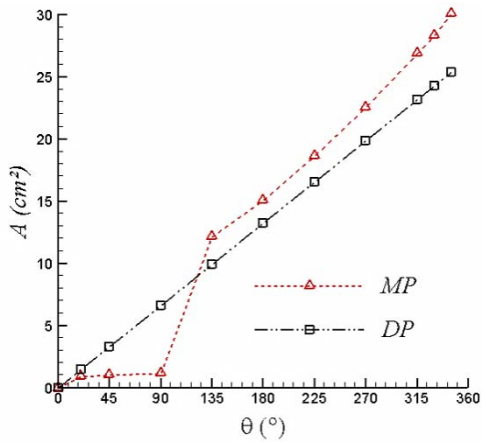


**Fig. 15. Variation of cross-section areas of the MP and DP volute.**

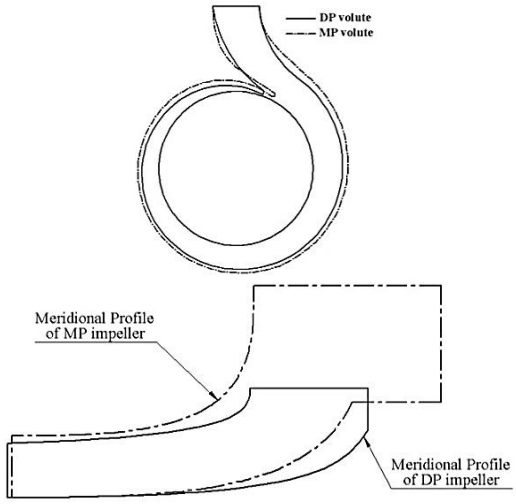


**Fig. 16. Meridional section of the impeller and volute profiles for the MP and DP.**

**Table 6 Design parameters of the MP and DP**

| Design Variables | Original | Designed |
|---|---|---|
| Impeller inlet diameter, (mm) | 115 | 108 |
| Impeller outlet diameter, (mm) | 264 | 266.5 |
| Blade inlet width, (mm) | 35.7 | 30.3 |
| Blade outlet width,(mm) | 19 | 16.7 |
| Inlet blade angle, (°) | 20.2 | 25.6 |
| Outlet blade angle, (°) | 16 | 13.5 |
| Impeller wrap angle (°) | 102.7 | 119.2 |
| Blade thickness (mm) | 5.1 | 4 |

### 3.4 Comparison of the Numerical Simulation Results for the MP and DP

The flow volume of the DP was numerically analyzed by CFD with the same boundary conditions and grid structure of the MP. Turbulence

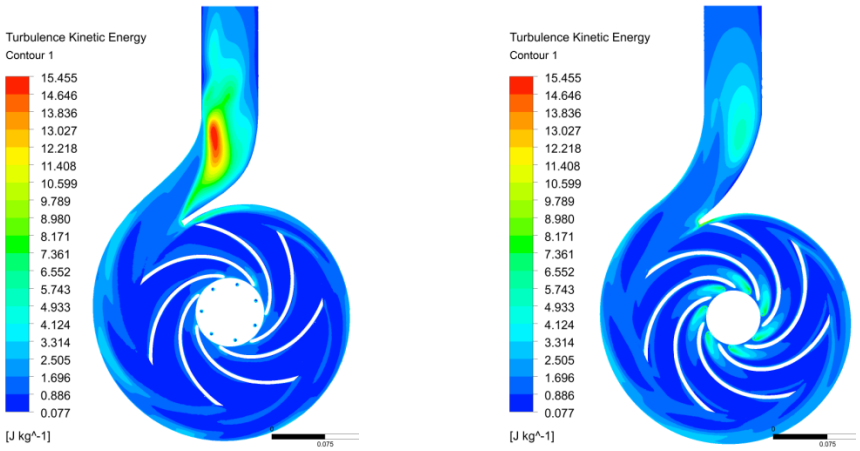


**Fig. 17. Turbulence kinetic energy distribution for the MP (left image) and the DP (right image) at mid-plane at100m$^3$/h flow rate.**

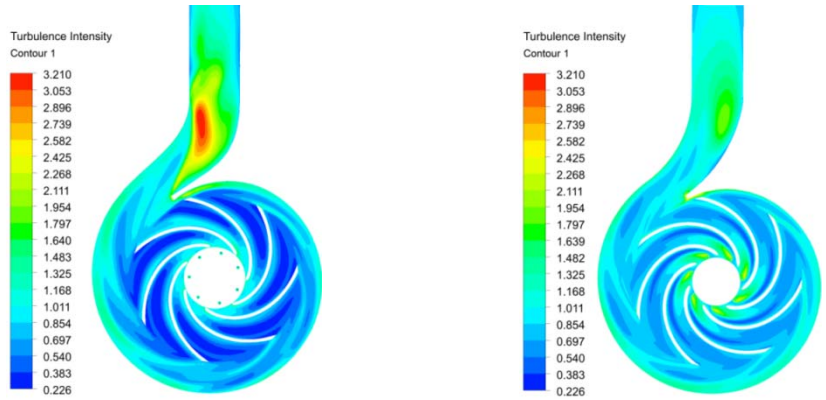


**Fig. 18. Turbulence intensity distributions for the MP (left image) and the DP (right image) at mid-plane and design flow rate of 100m$^3$/h.**

kinetic energy (TKE) and turbulence intensity distributions are given in Figs. 17 and 18.Reverse flow region in the volute of the MP was almost eliminated with geometrical modification in the DP. According to the new design distribution of TKE is significantly decreased as seen in Fig. 17. The maximum TKE value for the DP was decreased to 5 J/kg which was three times higher for the MP value of 15 J/kg. As seen in Fig. 17, turbulence intensity values in the outlet region of the volute for the MP was irregular and higher than the DP of the volute outlet. The maximum value of the turbulent intensity for the MP was 3.20% whereas that for the DP was only 2.0%.

Variation of the streamline patterns for the MP (left side images) and the DP (right side images) at mid-plane for the volume flow rate values of $Q/Q_d$=0.8, $Q/Q_d$=1 and $Q/Q_d$=1.35 are given in Fig. 19. Swirling flow and flow separation occur in the tongue and outlet pipe of the MP whereas this phenomenon has been diminished in the DP case. Flow separation is not observed in the flow passage between the impeller and volute of the DP. Because of the flow stream from the higher pressure side to lower one, foci are formed around the balance holes of the impeller for both the MP and the DP. Turbulence kinetic energy values in Fig. 17 have higher values around the balance holes which mean energy losses. Energy transmission from solid to fluid around the balance holes is also decreased. This energy loses arelessened in the case of the DP model, which requires lower shaft power. Variation of the parameter for the MP and DP for flow rate of $Q/Q_d = 1.0$ is presented in Table 7. As seen with improvements on the impeller and volute geometries hydraulic efficiency is increased in the DP since hydraulic torque is decreased. On the other hand, head of the DP is almost the same.

Figure 20 compares the numerical simulation results for the MP and the DP with the head and hydraulic efficiency versus volume flow rate. The head trends and values were very similar while the hydraulic efficiencies for the DP were greatly increased. On design condition, the heads of the MP and DP were found to be as 18m and 18.32 m and the hydraulic efficiency was increased from 55.98% to 63.09%.

## 4. CONCLUSIONS

In this study the following findings were obtained.

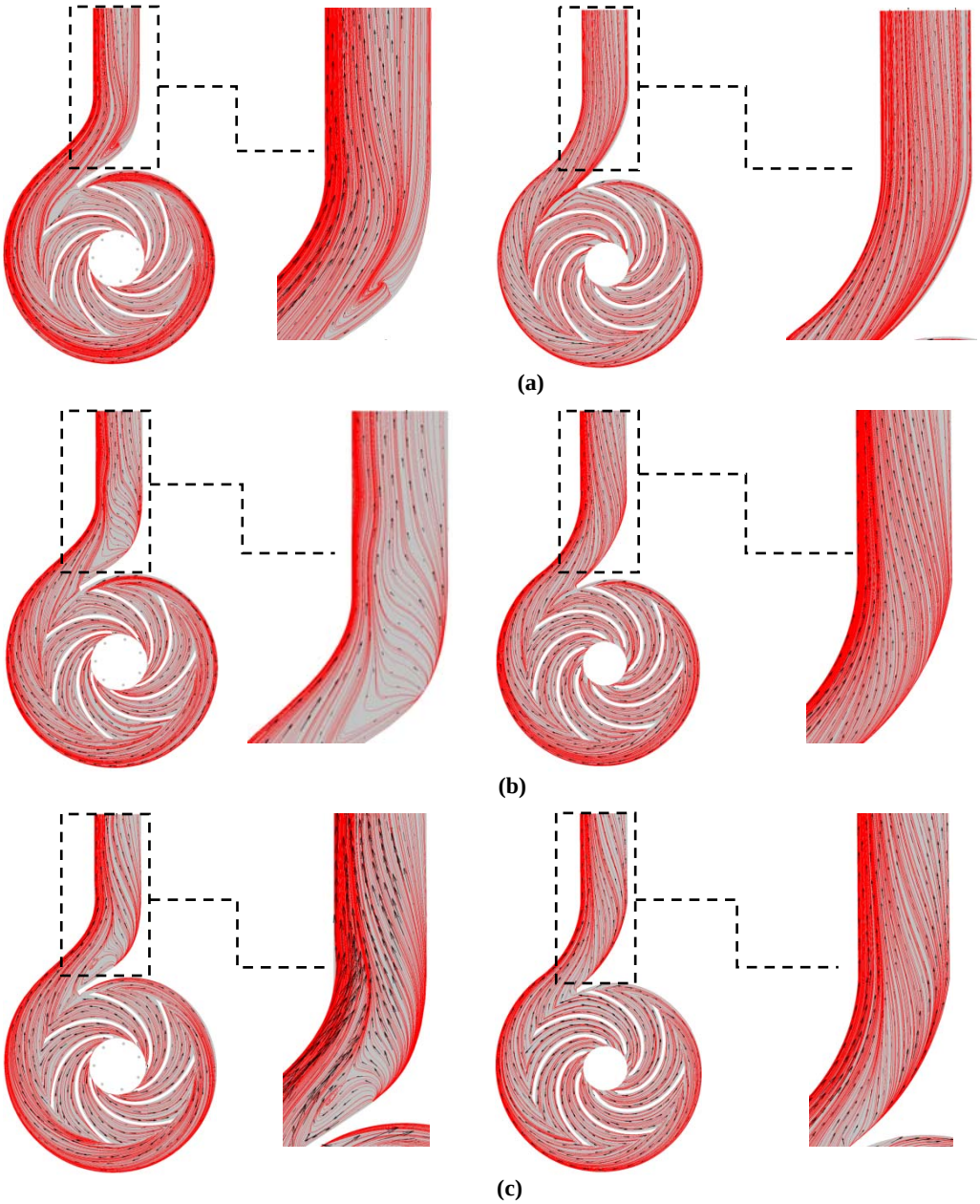


**Fig. 19. Variation of the streamline patterns for the MP (left side images) and the DP (right side images) at mid-plane for the volume flow rate values of a) $Q/Q_d = 0.8$,b)$Q/Q_d = 1$andc) $Q/Q_d = 1.35$.**

- Comparison of the MP and CMP showed that the head and hydraulic efficiency of the CMP were 15% and 18% larger, respectively on design flow rate.
- The surface roughness effect was analyzedby CFD. It was found that the hydraulic efficiency was decreased from 68% to 53% as the roughness value increases from 0 to 0.7 mm.
- The economic evaluation of the CMP application results in PBP is less than one year and %114 IRR ratio, which provides a high profit. In addition, the coating application protects the pump impeller and volute from corrosion and cavitation.
- It is revealed that the obtained experimental results are repeatable and reliable because of having very low uncertainty values around ± 1%.
- The deviation between the experimental and CFD results for the head and hydraulic efficiency values were found to be in the range of less than 10% for all flow rates and those values were respectively determined as 2.79% and 2.82% at design flow rate of 100$m^3$/h. This demonstrates that the applied CFD simulation could predict pump performance with an acceptable level. It was obtained that the reverse flow region in the MP considerably

affects the performance characteristics. For this reason, the impeller and the volute of the centrifugal pump were re-designed and numerically analyzed by taking reference the CFD and experimental results of the model pump. Finally, the hydraulic efficiency including the leakage losses and balance holes was increased in the ratio of %12.7. The head variation between the MP and the DP were in order of 18m and 18.3m at design flow rate. Despite this relatively small increment in head, hydraulic torque of the DP was calculated as 51.05 Nm while it was 56.62 Nm for the MP. This means that energy consumption of the pump can be decreased approximately 9.85%.

- In future, the DP pump can also be manufactured and experimentally tested. The DP can provide higher efficiency and head values when the wetted surfaces of the DP are coated with the polyurethane coating. Coating also obtains reduced vibrations and,consequently, reduced the stress of bearings and whole pump

**Table 7 The calculeted values for the MP and DP at flow rate ratio of the operation point at $Q/Q_d=1.0$**

| Parameters | MP | DP | Absolute relative difference (%) |
|---|---|---|---|
| Flow rate (m³/h) | 100 | 100 | - |
| Total pressure at the impeller inlet (kPa) | 56.96 | 56.29 | 1.19 |
| Total pressure at the impeller outlet (kPa) | 297.30 | 288.99 | 2.87 |
| Dynamic pressure at the impeller inlet (kPa) | 5.42 | 5.14 | 5.44 |
| Dynamic pressure at the impeller outlet (kPa) | 90.36 | 78.05 | 15.77 |
| Total hydraulic moment (Nm) | 55.78 | 51.53 | 8.24 |
| Hydraulic efficiency of the impeller (%) | 75.67 | 79.31 | 4.59 |
| Shaft power (kW) | 8.64 | 7.98 | 8.27 |
| Hydraulic power (kW) | 4.83 | 5.03 | 3.97 |
| Hydraulic efficiency of the pump (%) | 55.98 | 63.09 | 11.27 |

## ACKNOWLEDGEMENTS

This work is supported by SANTEZ program of the Ministry of Science, Industry and Technology of Turkey with number 01076.STZ.2011-2 and Selcuk University's Scientific Research Project Office Contract No: 13101009 and 14401075. The authors also would like to thank to the partner of the project Sempa Co. board (http://www.sempaltd.com/en/) to their support. This study is prepared by Osman Kocaaslan's Master of Science Thesis.

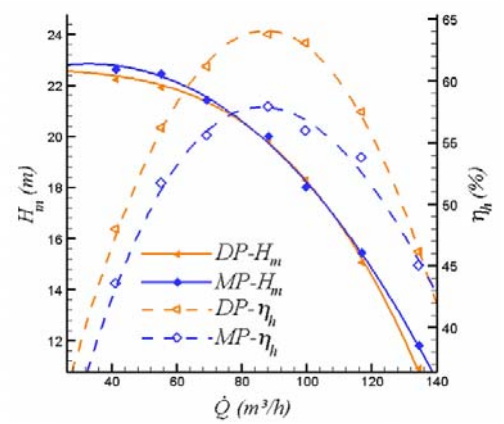


**Fig. 20. Variation of the head and hydraulic efficiency for the MP and DP.**

## REFERENCES

Anonymous,(2014)http://www.metaline.de/

Anonymous, Fluent 14.0 User Guide, Fluent Inc. (2015).

Babayigit, O., O. Kocaaslan, M.H. Aksoy, K.M. Güleren and M. Ozgoren (2015). Numerical identification of blade exit angle effect on the performance for a multistage centrifugal pump impeller. *European Physical Journal Web of Conferences*92, 02003.

Baysal, K. (1979). *Centrifugal Pumps*. Istanbul Technical University publishing house, Istanbul, Turkey. (in Turkish)

Bellary, S.A.I. and A. Samad (2013). Exit Blade Angle and Roughness Effect on Centrifugal Pump Performance, *ASME 2013 Gas Turbine India Conference, Bangalore*5–6.

Budris, A. R. (2012). Coatings Can Improve Pump Impeller Cavitation Damage Resistance. *WaterWorld*28 (4), 14.

Cengel Y. and J. Cimbala (2006). *Fluid Mechanics Fundamentals and Applications*. McGraw Hill, New York.

Dai J., Y. Wu and S. Cao (1997). Study on flows through centrifugal pump impeller by turbulent simulation. *Journal of Hydrodynamics, Ser. B*, 9(1), 11–23.

Golcu, M., Y. Pancar and Y. Sekmen (2006). Energy saving in a deep well pump with splitter blade. *Energy Conversion Management* 47(5), 638–651.

Gulich, J. F. (2014). *Centrifugal Pumps*, Springer-Verlag Berlin Heidelberg.

Holman J. P. (2001). *Experimental Methods for Engineers*, 7th ed., McGraw-Hill, New York.

Jafarzadeh, B., A. Hajari, M. M. Alishahi and H. M. Akbari (2010). The flow simulation of a low-specific-speed high- speed centrifugal pump. *App. Math. Modelling* 35, 242-249.

Kaya, M. and M. Aydın (2009). A Numerical Study for Evaluating Performance of Centrifugal Pump, *Global Conference on Global Warming (GCGW-09), 5-9 July 2009*, Istanbul-Turkey.

Kocaaslan, O, (2015). *Experimental and numerical investigation of an optimized pump impeller with polyurethane surface coating effect for efficiency improvement*, MSc thesis. Selcuk University, Konya, Turkey.

Kose, F., M. H. Aksoy and M. Ozgoren (2014). An Assessment of Wind Energy Potential to Meet Electricity Demand and Economic Feasibility in Konya, Turkey. *International Journal of Green Energy* 11, 559-576.

Li, W.G. (2011a). Blade Exit Angle Effects on Performance of a Standard Industrial Centrifugal Oil Pump. *Journal of Applied Fluid Mechanics* 4, 105-119.

Li, W. G. (2011b). Effect of exit blade angle, viscosity and roughness in centrifugal pumps investigated by CFD computation, *Task Quarterly* 15(1), 21-41.

Maillard, J. (2008). *Coating Technology Increases Pump Performance*. Belzona Polymerics Ltd, Claro Road, Harrogate, North Yorkshire HG1 4DS.

Ozerdem, B., S. Ozer and M. Tosun (2006). Feasibility study of wind farms: a case study for Izmir. *Journal of Wind Engineering and Industrial Aerodynamics* 94, 725-743.

Perez J., S. Chiva, W. Segala, R. Morales, C. Negrao, E. Julia and L. Hernandez (2010). Performance analysis of flow in a impeller-diffuser centrifugal pumps using CFD: Simulation and experimental data comparisons, *European Conference on Computational Fluid Dynamics ECCOMAS CFD 2010*, Lisbon, Portugal, 1-18.

Stepanoff, A. J. (1957). *Centrifugal and axial flow pumps*. John Wiley and Sons, New York.

Xia, W. (2002). Polymer Coating of Pumps Boosts Efficiency, Performance.*Water World*.

Yang S. S., S. Derakshan and F.Y. Kong (2012). Theoretical, numerical and experimental prediction of pump as turbine performance. *Renewable Energy* 48,507-513.

Zhou, L, W. Shi, W. Lu, B. Hu and S. Wu (2012). Numerical investigations and performance experiments of a deep-well centrifugal pump with different Diffusers. *Journal of Fluids Engineering* 134(7), 071102-071108.